Structural Engineering and Mechanics, *Vol. 57, No. 4 (2016) 657-680*
DOI: http://dx.doi.org/10.12989/sem.2016.57.4.657

Shear strength estimation of RC deep beams using the ANN and strut-and-tie approaches

Gunnur Yavuz*

Engineering Faculty, Department of Civil Engineering, Selcuk University, Konya, Turkey

(Received April 18, 2014, Revised December 7, 2015, Accepted January 15, 2016)

Abstract. Reinforced concrete (RC) deep beams are structural members that predominantly fail in shear. Therefore, determining the shear strength of these types of beams is very important. The strut-and-tie method is commonly used to design deep beams, and this method has been adopted in many building codes (ACI318-14, Eurocode 2-2004, CSA A23.3-2004). In this study, the efficiency of artificial neural networks (ANNs) in predicting the shear strength of RC deep beams is investigated as a different approach to the strut-and-tie method. An ANN model was developed using experimental data for 214 normal and high-strength concrete deep beams from an existing literature database. Seven different input parameters affecting the shear strength of the RC deep beams were selected to create the ANN structure. Each parameter was arranged as an input vector and a corresponding output vector that includes the shear strength of the RC deep beam. The ANN model was trained and tested using a multi-layered back-propagation method. The most convenient ANN algorithm was determined as trainGDX. Additionally, the results in the existing literature and the accuracy of the strut-and-tie model in ACI318-14 in predicting the shear strength of the RC deep beams were investigated using the same test data. The study shows that the ANN model provides acceptable predictions of the ultimate shear strength of RC deep beams (maximum $R^2 \approx 0.97$). Additionally, the ANN model is shown to provide more accurate predictions of the shear capacity than all the other computed methods in this study. The ACI318-14-STM method was very conservative, as expected. Moreover, the study shows that the proposed ANN model predicts the shear strengths of RC deep beams better than does the strut-and-tie model approaches.

Keywords: artificial neural network; deep beam; shear strength; strut-and-tie model; reinforced concrete

1. Introduction

Reinforced concrete (RC) deep beams are structural members that are under the effect of disturbed stress trajectories (i.e., *D* regions). The classical elastic theory of bending is not valid in D regions, and the design of the deep beams is intended to consider the shear effect. These structural members are used in tall buildings, offshore gravity structures, transfer girders, pile caps, folded plates, and foundation walls. The load carrying capacity of a deep beam depends on the strength of the compressive strut that joins the loading point and the support reaction point (Eun *et al.* 2006).

*Corresponding author, Assistant Professor, E-mail: gyavuz@selcuk.edu.tr

http://www.techno-press.org/?journal=sem&subpage=8 ISSN: 1225-4568 (Print), 1598-6217 (Online)

The ultimate shear strength of deep beams can be determined using various methods. The strut-and-tie method is commonly used to compute the deep beams, and this method has been adopted in many building codes (ACI318-14, Eurocode 2-2004, CSA A23.3-2004). Also, different shear strength prediction methods of RC deep beams were investigated (Mohammadhassani *et al.* 2015, Chetchotisak *et al.* 2014). The strut-and-tie model is a rational and effective method for solving structural members that have statically or geometrically discontinuous regions (i.e., concentrated load or corner of frames, corbels, deep beams and openings). The internal forces in discontinuity regions can be modeled using a strut-and-tie model consisting of concrete compression struts, steel tension ties and joints referred to as nodal zones (MacGregor 1997). This model considers the load path in a structure and accepts that RC members carry loads through distributed compression stress areas (compression struts) and tension stress areas (tension ties) (Schlaich *et al.* 1987).

Artificial neural networks (ANNs) represent one of the artificial intelligence applications that have been implemented by engineers in particular to perform design tasks. ANNs are applied to perform many different tasks, including the prediction of function approximation, classification, and filtering (Arslan 2010). ANNs have been successfully applied to a number of areas in civil and structural engineering applications. In recent literature; structural analysis and design, structural dynamics and control, structural damage assessment, the evaluation of earthquake performance of reinforced concrete and steel structures are good examples of the application of ANNs in structural engineering (Arslan 2009, Arslan *et al.* 2007, Inel 2007, Chen *et al.* 1995, Elcordy *et al.* 1993, Lautour and Omenzetter 2009, Akbas 2006, Ozturk 2012, Yavuz *et al.* 2014).

In this study, the use of ANN models to predict the shear strength of RC deep beams and to evaluate the accuracy of the building code approaches in predicting the shear capacity of RC deep beams is performed. In this study, the experimental data for 214 RC deep beams were selected from the existing database published by Park and Kuchma (2007). Using their experimental results, the back-propagation algorithm was performed for the training on the shear strength of RC deep beams. Additionally, the training error, test error, and correlation coefficient (R^2), which indicate the initial performance evaluation of the back-propagation algorithm, were compared. Furthermore, ACI318-14 building code strut-and-tie model (ACI318-14-STM) approaches and existing literature (EL) (Park and Kuchma 2007) results were examined by comparing their predictions with the data of the experimental studies results. The results obtained by the ANN model and strut-and-tie model (STM) approaches were compared with each other. In this study, the strut-and-tie design methods in the ACI318-14 code formulas and the ANN results were compared and evaluated. In the EL study, a different strut-and-tie model approach was developed for calculating the capacity of reinforced concrete deep beams and their effectiveness.

2. Determining the shear strength of deep beams

Two calculation methods to determine the shear strength of reinforced concrete deep beams are suggested in ACI318-14: Deep beams shall be designed either by considering the nonlinear distribution of strain or by chapter 23 of ACI318-14. The shear strength V_n for the deep beam should not be greater than Eq. (1).

$$V_n = \phi 10\sqrt{f_c^{'}}\, b_w d \tag{1}$$

In Eq. (1), ϕ is strength reduction factor, $f_c^{'}$ is the specified concrete compressive strength, b_w is

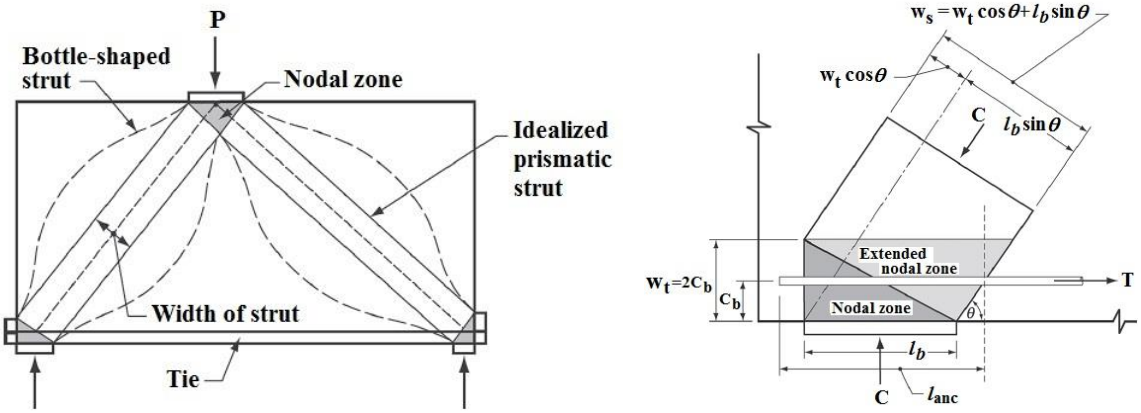

(a) Schematic view of strut-and-tie model (b) Extended nodal zone

Fig. 1 Components of a typical strut-and-tie model of a deep beam (ACI318-14)

the beam web width and d is the effective depth.

Another computational method for deep beams in ACI318-14 is the strut-and-tie model (ACI318-14-STM). This model consists of concrete compressive struts and reinforcing bars as tension ties and nodal zones. A strut-and-tie model is a system of forces in equilibrium with a given set of loads (MacGregor 1997).

A schematic view of the strut-and-tie model of a deep beam and the extended nodal zone showing the effect of the distribution of the forces is shown in Fig. 1. By using ACI318-14-chapter 23, designers can select the shape and dimensions of the load-resisting strut-and-tie model. Generally, more than one strut-and-tie model can be used. It is important to determine optimal load path and section types and properties of the strut and tie members in the D regions. If an unsuitable strut-and-tie model is selected, significant cracks and the local crushing on the concrete under service loads and the inadequate strength to support will occur (Park and Kuchma 2007).

The shear capacity of the deep beams V_n is determined with Eq. (2) according to the ACI318-14, chapter 23.

$$V_n = 0.85\beta_s f_c' b_w w_s \sin\theta_s \tag{2}$$

In Eq. (2), β_s values are 1.0 for struts with uniform cross-sectional area along length, 0.75 or 0.60λ for bottle shaped struts, 0.40 for struts in tension members or the tension zones of members, 0.60λ for other cases and λ=1.0 for normal weight concrete. Additionally, β_s values can be determined by web reinforcement ratio for a bottle shaped strut (ACI318-14). In this case β_s=0.75 for beams with web reinforcement ratio with $\sum \frac{A_{si}}{b_s s_i} \sin\alpha_i \geq 0.003$ and otherwise

$$\beta_s = 0.6\lambda \tag{3}$$

$$\tan\theta_s = jd/a; \quad jd = h - c - w_t'/2; \quad w_s = (w_t \cos\theta_s + l_b \sin\theta_s) \tag{4}$$

In the above equations, f_c' is the specified concrete compressive strength, b_w is the beam web width, w_s is the width of the concrete strut, θ_s is the concrete strut angle, A_{si} is the area of

reinforcement crossing the strut, s_i is the spacing of the reinforcement crossing the strut, α_i is the angle of the reinforcing bar, *jd* is the distance between the center of the top and bottom nodes, a is the shear span, h is the height of the beam, *c* is the concrete cover, w_t is the depth of the bottom node, and l_b is the width of the support bearing plates. In this study, simply supported beams have been considered. Accordingly, the values in Eq. (3) and (4) were used to calculate the shear capacity values V_n.

These ACI318-14-chapter 23 code formulae showed that the shear strength computed by the strut-and-tie models is greatly dependent on the width and inclination of the compressive struts, the effective strength of the concrete and the amount of web reinforcement. In addition, the effectiveness factor of the concrete in ACI318 is 0.6 or 0.75 depending on the amount of web reinforcement and the independent of concrete strength and the shear span-to-overall depth ratio (Yang *et al.* 2008).

Results similar to the experimental values were obtained by the existing literature (EL) method (i.e., strut-and-tie based method) versus the ACI318-05 code. In EL, the proposed approach is a compatibility-based strut-and-tie method that considers the effects of compression softening of the cracked concrete. The EL-developed model offers a new approach for the use of compatibility-based strut-and-tie methods (Park and Kuchma 2007).

3. Selection of database

In the literature, there are extensive available experimental data on the behavior of the RC deep beams. The tests were performed under similar loading types, and the selected parameters in these tests were similar. The experimental data considered in this study was obtained from Park and Kuchma (2007) and included the test results for 214 RC deep beams. Park and Kuchma (2007) present a strut-and-tie-based method for calculating the strength of normal and high strength reinforced concrete deep beams. The test specimens were of solid rectangular deep beams. Typical loading system and tested deep beams are shown in Fig. 2. This database is sufficiently large to enable a fair critique of the code provisions and the validation of the proposed model according to Park and Kuchma (2007). The parameters affecting the strength of the RC deep beams were considered to be the dimensions of the cross section, the shear span-to-depth ratios (*a/d*), the compressive strength of the concrete, the ratio of longitudinal reinforcement and the ratios of

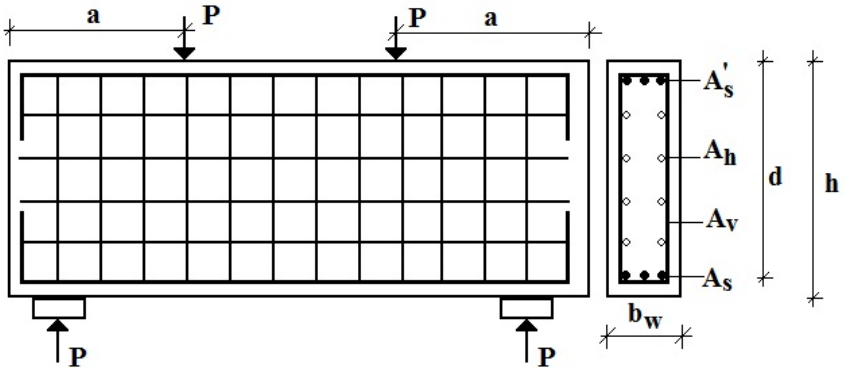

Fig. 2 Typical loading system and tested deep beams

Table 1 Range of parameters

Parameters	Identification	Range	
		Min	Max
h (mm)	overall height of deep beam	254	915
b (mm)	width of deep beam	76	305
d (mm)	effective depth of deep beam	216	801
a (mm)	shear span	125	1250
a/d	aspect ratio	0.27	2.7
f_c' (MPa)	compressive strength of the concrete	13.8	73.6
ρ (%)	ratio of longitudinal reinforcement	0.52	4.08
ρ_h (%)	ratio of horizontal web reinforcement	0	2.45
ρ_v (%)	ratio of vertical web reinforcement	0	2.65

horizontal and vertical web reinforcements. The deep beams in this literature (Park and Kuchma, 2007) include concrete compressive strengths ranging from 13.8 MPa to 73.6 MPa, *a/d* shear span-to-depth ratios ranging from 0.27 to 2.7, ratios of longitudinal reinforcement ranging from 0.0052 to 0.0408, ratios of horizontal web reinforcement ranging from 0 to 0.0245, and ratios of vertical web reinforcement ranging from 0 to 0.0265. As shown in Table 1, a total of 214 tests satisfy the variables mentioned above.

4. Fundamental aspects of artificial neural networks

The use of ANNs ensures an alternative approach to predict the shear strength of RC deep beams. A multilayer perceptron neural network (MLP NN) is a feed-forward neural network model (Yavuz *et al.* 2014). The MLP model consists of one input layer, one or more hidden layer(s), and one output layer (Fu 1994). The structure of the ANNs used in this study is provided in Fig. 3. The neurons of a layer are fully connected to the neurons of the neighboring layers with weights. The initial values of these weights are randomly assigned as small real values. The outputs of the hidden layer and the output layer neurons are calculated with defined transfer functions (Yavuz *et al.* 2014). In this study, the ANN architecture consisted of seven input neurons and one output neuron, and a two-layered feed-forward neural network model was used and trained with the error back-propagation method. In engineering problems, the number of input and output parameters is generally determined by design requirements (Arslan 2010). However, the selection of the number of hidden layer neurons is entrusted to the user. There is no general rule for selecting the number of neurons in a hidden layer (Arslan 2009, Arslan *et al.* 2007). The back-propagation learning algorithm can be used to train the MLP network. Therefore, these weights are adjusted for a given set of input-output pairs (Rumelhart *et al.* 1986). The mean squared error (MSE %) can be used to appraise the performance of the ANN model according to number of hidden neurons (Eq. (5)).

$$MSE = \frac{1}{n}\sum_{i=1}^{n}(Y_i - Y_i^{'})^2 \tag{5}$$

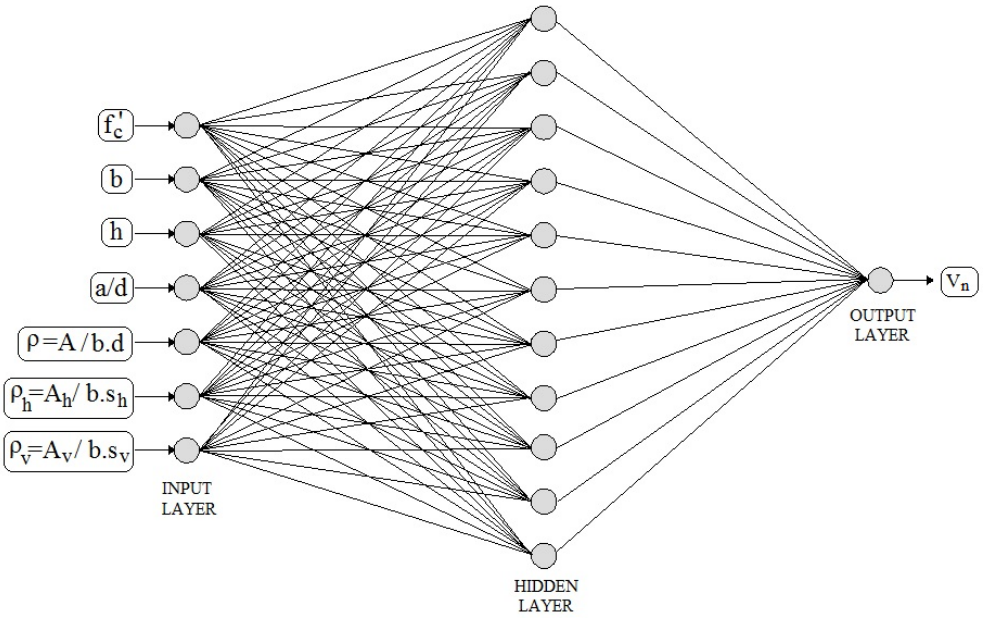

Fig. 3 Architecture of the selected ANN model

In this equation, n is the number of samples in the training or testing data. Y_i is the desired output, and Y_i' is the output of the neural network. In this study, the ANNs were developed using the MATLAB software package (MATLAB version 7.10.0 with a neural networks toolbox). The input data were normalized in the range of [-1 1], and the output data were normalized in the range of [0 1]. Data scaling (normalization) is an important phase for network training. Input and output data are normalized before using them in the network. Simple linear normalization functions were applied to the data using Eq. (6).

$$S_x = 2\frac{(X - X_{\min})}{(X_{\max} - X_{\min})} - 1 \quad (\text{for } [-1\ 1]); \qquad S_x = \frac{(X - X_{\min})}{(X_{\max} - X_{\min})} \quad (\text{for } [0\ 1]) \tag{6}$$

In this equation, S_x is the normalized value of the variable X, and $X_{\min}$ and $X_{\max}$ are the minimum and maximum values of the variables, respectively.

In this study, a hyperbolic tangent sigmoid transfer function was selected on the hidden layer, and a sigmoid transfer function was utilized on the output layer. A training function trainGDX was used; this function updates weight and bias values according to the gradient descent momentum and an adaptive learning rate. The performance of the network was very sensitive to the learning rate (l_r) and was held constant throughout the training for standard back-propagation. For the training process, the maximum training cycles, learning rate (l_r), and momentum coefficient (m_c) selected were 1000, 0.1 and 0.9, respectively. The MSE is used as a performance function to evaluate the best number of hidden neurons. The ANN architecture consisted of seven input neurons covering the geometrical and material properties of the deep beams and one output neuron covering the shear strength (Fig. 3). The number of neurons in the hidden layer was varied from 10 to 100 to obtain the best result. The total data set contained 214x8 datasets. The data set was divided equally into training and testing data sets (107 data sets). The parameter combination that

Table 2 The optimum network parameters

Parameter	Value
Number of training data	107
Number of testing data	107
Maximum epoch number	1000
Learning rate (l_r)	0.1
Momentum coefficient (m_c)	0.9
ANN structure	7:HN:1
Number of hidden neurons (best)	60
R^2 (training)	0.9855
R^2 (testing)	0.9711

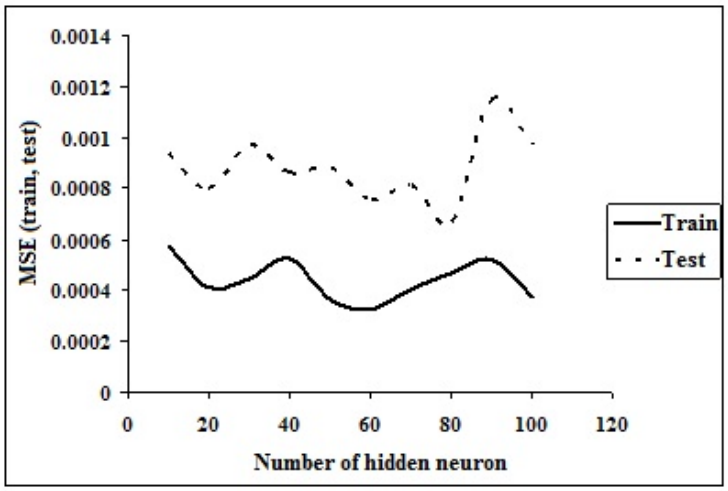

Fig. 4 Training and testing errors corresponding to number of hidden layer neurons

resulted in the best average of the training and testing performances was selected as the best one for the corresponding model. The optimum parameter combination is shown in Table 2. The study shows that the ANN model provides reasonable predictions for the shear strength of the RC deep beams ($R^2 \approx 0.97$).

5. Results and discussion

5.1 The ANN model results

In this study, 7:HN:1 ANN structures were used for the strength for the input values of f_c', b, h, a/d, ρ, ρ_h and ρ_v as well as for the output values of the strength capacities of the RC deep beams as V_n. The performance values of the GDX back-propagation method that are related to the determination of the shear strength of the RC deep beams are provided in Table 2. The changes in the training and testing errors corresponding to the number of hidden layer neurons are shown in Fig. 4.

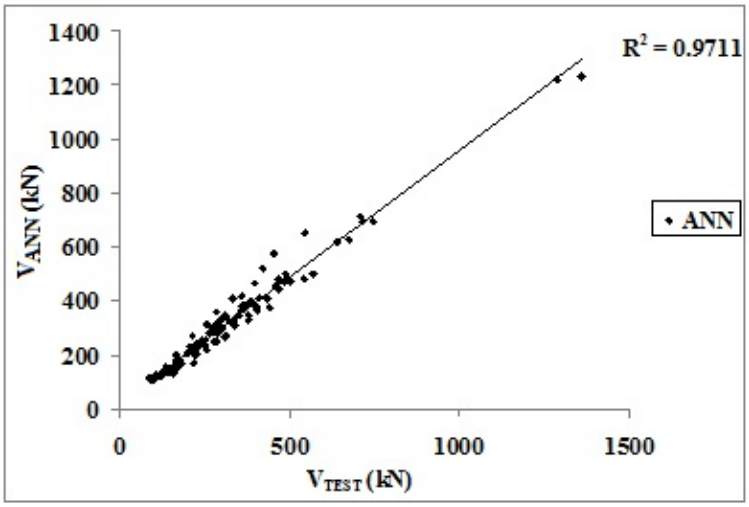

Fig. 5 Performance of the ANN model in estimating the shear strength capacity of the deep beams for testing data

A general investigation was performed to evaluate success of the ANN model by considering Table 2 and Fig. 4. Performance of the ANN model in estimating the shear strength capacity of the deep beams for testing data is shown in Fig. 5 in accordance with the correlation coefficient (R^2). The back-propagation method obtained a 97% averaged accuracy rate (100%-error%) for the test phase of the neural network. Also, average values of V_{test}/V_{ANN} for each of the reference works are presented in Table 3. Different architectures of the ANN model have the ability to solve this problem. The training time should not be considered as a significant performance property because this study is not a "real time" application. The selection of the data used in the training set and algorithm directly affected the accuracy and the rate. Therefore, the selection of the most appropriate algorithm for each data set is an important factor in the solution of the problem. The success of the ANN training algorithm depends on the data set and the structure of the network. The selected ANN model presented above is valid only for the ranges of databases provided in the Appendix Table. In the study, by selecting a different number of hidden nodes (HN) between 10 and 100 for the hidden layer, the optimum number of nodes was determined by applying separate solutions for each node. Fixing the number of nodes of the hidden layer requires many trials. The important factors affecting the success of the application are the number of hidden layer neurons, the iteration number, the learning rate, the momentum coefficient parameters and the learning algorithm. Each parameter affects the performances during the solution of the problem because of their different properties. In this study, the optimum number of hidden layer neuron was determined as 60 neurons.

5.2 Building code (ACI318-14-STM) and EL results

To analyze the accuracy of the other two methods for the strength of the RC deep beams, the test results provided in the Appendix Table were compared with the results of the other conventional (EL) and ACI318-14-STM code approaches. Performances of the ACI318-14-STM method and EL in estimating the shear strength capacity of the deep beams for all data are shown

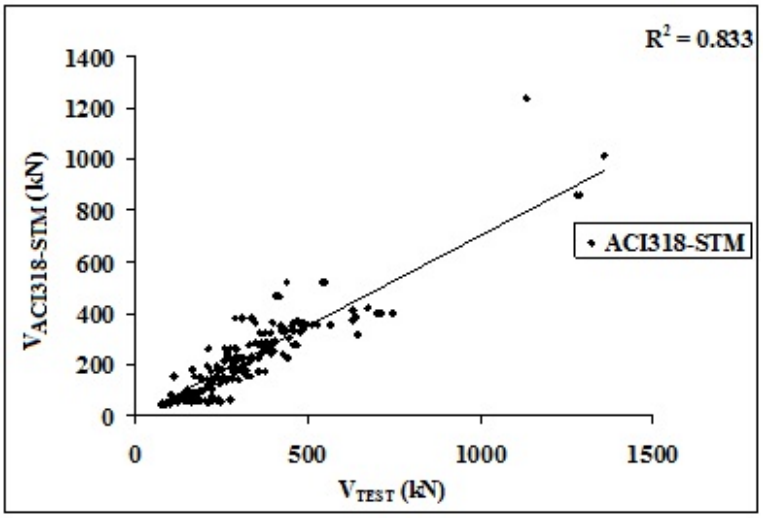

Fig. 6 Performance of the ACI318-14-STM method in estimating the shear strength capacity of the deep beams for all data

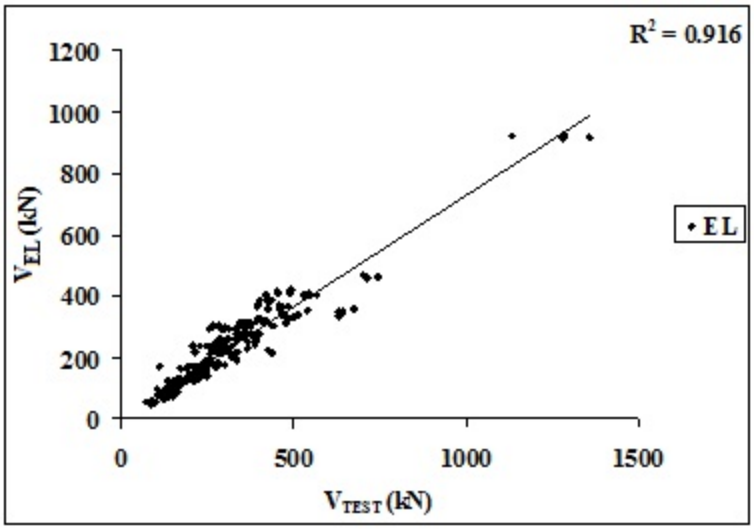

Fig. 7 Performance of the EL method estimating the shear strength capacity of the deep beams for all data

in Figs. 6-7, respectively. The prediction capability results of the ACI code and EL related to the strength of the RC deep beams for the 214 tested specimens are presented in Table 3.

The minimum, maximum and average values of the selected parameters (f_c', a/d, ρ_h and ρ_v) for the reference studies and the average values of $V_{n,test}/V_{n,computed}$ for each of the reference works are presented in Table 3. In the specimens that have horizontal and/or vertical web reinforcement ratios of less than 0.003, it was shown that the ACI318-14-STM and EL results were closer to the experimental shear strengths (Table 3).

The results closest to the experimental shear strengths were determined for the specimens that have high strength concrete and an average concrete compressive strength that is greater than 40

Table 3 Minimum, maximum and average values of the selected parameters from the reference studies and average values of $V_{n,test}/V_{n,comp.}$

Reference		Minimum, maximum and average values of specimen properties				Average values of $V_{n,test}/V_{n,comp.}$		
		f_c' (MPa)	a/d	ρ_h (%)	ρ_v (%)	$V_{test}/V_{ACISTM-318}$	V_{test}/V_{EL}	$V_{test}/V_{ANN-all\ data}$
Smith and Vantsiotis (1982)	Min.	16.1	1.00	0	0			
	Max.	22.7	2.08	0.91	1.25	2.00	1.54	1.01
	Ave.	19.7	1.29	0.49	0.49			
Kong *et al.* (1970)	Min.	18.6	0.35	0	0			
	Max.	24.6	1.18	2.45	2.45	3.11	1.59	0.97
	Ave.	21.1	0.65	0.78	0.78			
Clark (1951)	Min.	13.8	1.17	0	0.34			
	Max.	47.6	2.34	0	1.22	1.65	1.29	1.00
	Ave.	26.2	1.64	0	0.50			
Oh and Shin (2001)	Min.	23.7	0.50	0	0			
	Max.	73.6	2.00	0.94	0.37	1.29	1.28	0.98
	Ave.	51.6	1.02	0.39	0.16			
Aguilar *et al.* (2002)	Min.	28.0	1.14	0	0.10			
	Max.	32.0	1.27	0.13	0.31	1.30	1.38	1.04
	Ave.	30.0	1.18	0.13	0.26			
Quintero-Febres *et al.* (2006)	Min.	22.0	0.81	0	0			
	Max.	50.3	1.57	0.15	0.67	1.40	1.28	1.01
	Ave.	34.9	1.15	0.06	0.17			
Tan *et al.* (1995)	Min.	41.1	0.27	0	0.48			
	Max.	57.3	2.70	0	0.48	1.39	1.38	1.02
	Ave.	49.3	0.99	0	0.48			
Anderson and Ramirez (1989)	Min.	27.5	2.15	0	2.65			
	Max.	42.7	2.15	0	2.65	1.48	1.57	0.98
	Ave.	33.8	2.15	0	2.65			

MPa in the Oh and Shin (2001) studies and the Tan *et al.* (1995) studies. As shown in Table 3, $V_{n,test}/V_{n,comp.}$ values increased greatly for the studies containing a low average concrete compressive strength. $V_{n,test}/V_{n,comp.}$ values were close to the experimental results for the specimens that have an average a/d ratio that is approximately 1.

5.3 Comparison of the ANN model, strut-and-tie model equations and existing literature

The predictions of the shear capacities of the RC deep beams for the proposed ANN model and the predictions of the ACI318-14-STM model as explained in Section 2 were compared with the compiled experimental database in the Appendix Table. Comparable figures of the target values,

obtained neural networks, building code and existing literature outputs are shown in Figs. 5-7. In these figures, a comparison of the experimental values and the estimated shear strength is plotted. According to the results shown in Figs. 5-7, the algorithm produced better estimates than the other conventional (EL) and ACI318-14-STM code approaches in accordance with the correlation coefficient (R^2). Because the proposed ANN model estimated the shear capacities of the RC deep beams with an approximately 97% accuracy, the results obtained through the proposed ANN model and the EL results were very close. Additionally, due to several assumptions made for the simplification of the conventional approaches, the estimation capacities of the conventional approaches were lower than those obtained by the ANN approach. When more comprehensive analysis assumptions are made in the conventional approach, better estimations become possible but may increase the complexity of the analysis, whereas the ANN approach can lead to reliable results without excessive complexity.

In this study, the root mean squared error (RMSE), mean absolute error (MAE) and mean absolute percentage error (MAPE) performance parameters were then used to appraise the performance of the methods. The RMSE, MAE and MAPE performance parameters were computed by Eqs. (7), (8) and (9), respectively.

$$RMSE = \sqrt{\frac{1}{n}\sum_{i=1}^{n}(Y_i - Y_i^{'})^2} \tag{7}$$

$$MAE = \frac{1}{n}\sum_{i=1}^{n}\left|Y_i - Y_i^{'}\right| \tag{8}$$

$$MAPE = \frac{1}{n}\sum_{i=1}^{n}\left|\frac{Y_i - Y_i^{'}}{Y_i}\right| \tag{9}$$

In the above equations, n is the number of samples in the training or testing data; Y_i is the desired output (measured values); and Y_i' is the estimated output of the neural networks and other methods (simulated values of the ANN, EL and ACI318-14-STM code approach). The performance parameters for the applied methods are given in Table 4. From Table 4, the ANN model displayed the best performance when analyzing the R^2, MSE, MAE and MAPE parameters.

A comparison of the ANN results derived from the GDX algorithm approach with the aforementioned code approaches derived from ACI318-STM that provides very high correlation

Table 4 Performance results of the prediction methods

	R^2	RMSE	MAPE	MAE
ANN-train	0.985	23.136	0.071	16.952
ANN-test*	0.971	35.250	0.082	24.336
ACI318-STM*	0.862	128.057	0.380	105.090
EL*	0.918	112.007	0.273	82.914
ACI318-STM-all data	0.833	126.679	0.385	105.367
EL-all data	0.916	108.015	0.275	82.082

Note: *Performance values were computed for the test stage results of the model.

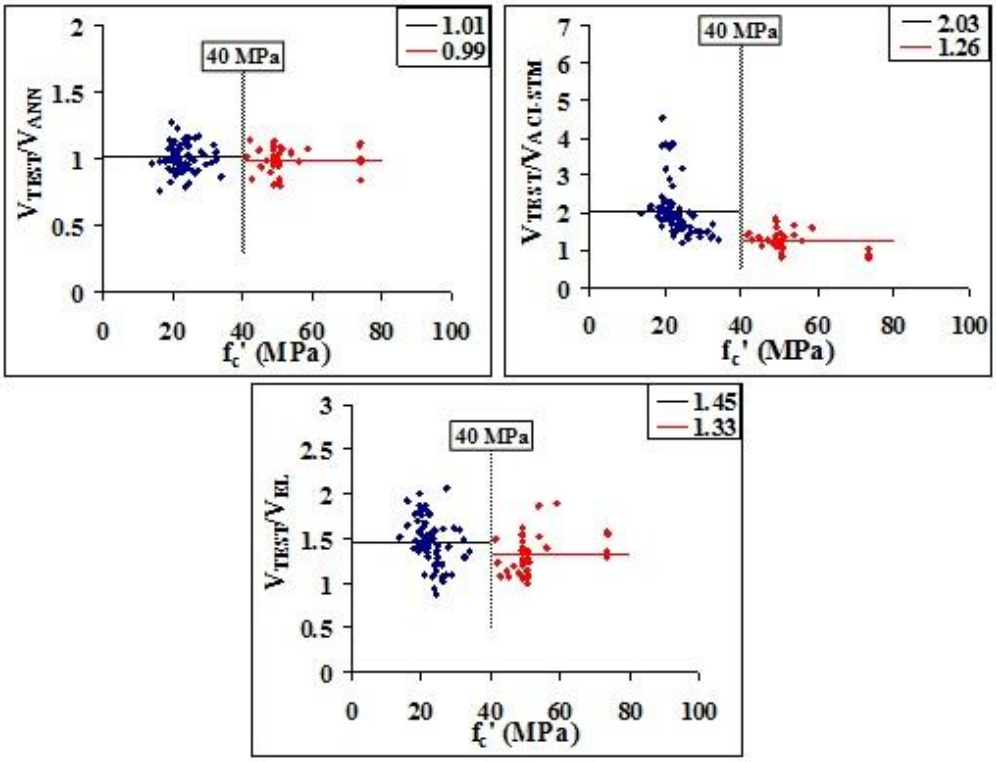

Fig. 8 Effect of the parameter f_c' on the shear strength of the RC deep beams

coefficients (R^2) for the training and testing data was performed. In this study, the shear span-to-depth ratio (a/d), the compressive strength of concrete (f_c'), the horizontal shear reinforcement ratio ρ_h and the vertical shear reinforcement ratio ρ_v were selected as the effective parameters on the shear strength of the deep beams to compare the aforementioned methods with each other. Figs. 8-11 show the errors that are induced by the discrepancy of the f_c', a/d, $\rho_h=A_h/b.s_h$ and $\rho_v=A_v/b.s_v$ parameters between the test-ANN model, the test-EL and the test-ACI-STM. In these figures, test stage values were considered for ANN results. The wide ranges of parameters are effective on the strength behavior of the RC deep beams. Therefore, all the parameters selected should be considered. The effect of the concrete compressive strength on the shear strength of the deep beams is shown in Fig. 8. The closest results were obtained for deep beams having 40 MPa and higher strength concrete. a/d is the shear span-to-effective-depth ratio, which plays an important role in the failure type and the cracking pattern for the deep beams. Its effect on beam behavior is shown in Fig. 9. ρ_h and ρ_v are the ratio of the horizontal and vertical web reinforcement, and their effects on the shear strength are shown in Figs. 10-11, respectively. In this study, the limit values were determined to understand the effects of the parameters clearly.

The selected limit values were 40 MPa for the concrete compressive strength f_c', 2 for the aspect ratio (a/d), and 0.003 for the horizontal (ρ_h) and vertical (ρ_v) web reinforcement ratio. The average ratios of the experimental shear strengths to the computed shear strengths according to the aforementioned methods ($V_{ntest}/V_{ncomp.}$) are provided in Table 5 and considered the specified limit values in point of the f_c', a/d, ρ_h, ρ_v parameters for the specimens.

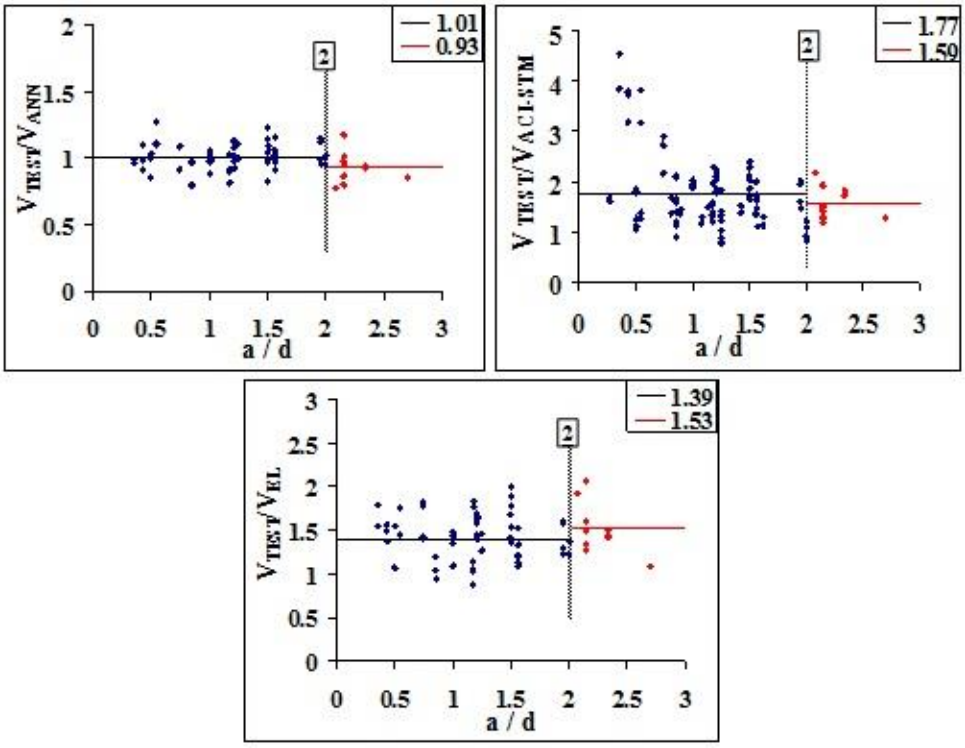

Fig. 9 Effect of the parameter a/d on the shear strength of the RC deep beams

Table 5 $V_{n,test}/V_{n,comp.}$ ratios

Method	f_c' (MPa)		*a/d*		ρ_h		ρ_v	
	≤ 40	> 40	≤ 2	> 2	≤ 0.003	> 0.003	≤ 0.003	> 0.003
ANN-test data	1.01	0.99	1.01	0.93	0.97	1.00	0.99	1.00
ACI318-STM	2.03	1.26	1.77	1.59	1.64	1.82	1.65	1.82
EL	1.45	1.33	1.39	1.53	1.34	1.43	1.36	1.44

When considering the ratios in Table 5, strength values closer to those of the test results were obtained for the test specimens with high strength concrete (f_c'>40 MPa) when using the EL and ACI318-14-STM method. However, a ∓1% difference from test results was obtained by the ANN model for all concrete compressive strength values. As a result of the general comparison, strength values very close to the experimental results were obtained by the ANN model for all selected parameters. Hence, the results obtained from the EL and ACI318-14-STM methods are very close to each other for high-strength concrete, according to the average ratios. When examining the average ratios at the upper and lower boundary of the limit values for each method, 2%, 12% and 77% differences were obtained for the ANN, EL and ACI318-14-STM methods, respectively (Fig. 8).

When examining the *a/d* aspect ratios, the most convenient values with test results were obtained by the ANN model. Additionally, a greater average ratio difference was computed for *a/d*>2 according to the ANN model. When comparing the methods on their own, the ANN model

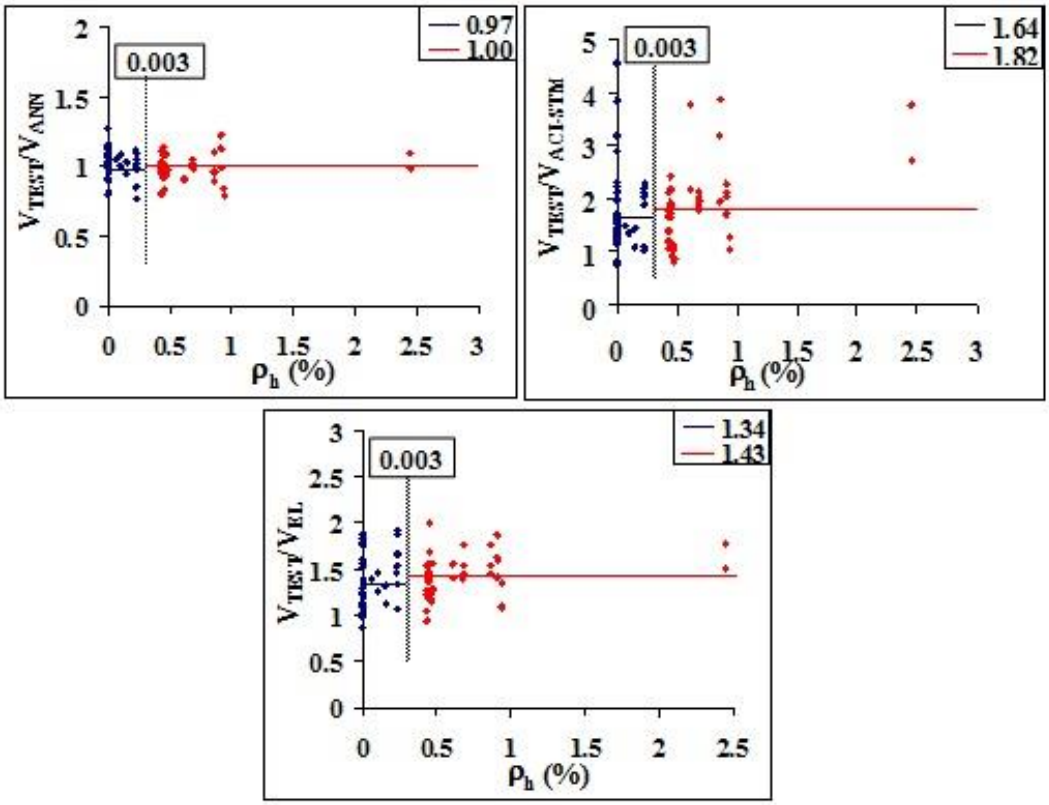

Fig. 10 Effect of the parameter ρ_h on the shear strength of the RC deep beams

and the EL method provide improved results in the a/d<2 specimens. At the same time, fewer differences in the average ratio were determined in the a/d>2 specimens according to the ACI318-STM method. According to these results, the ANN model and the EL method provide a lower error rate for deep beams that have very small aspect ratios. The shear effect is very important in deep beams that have small aspect ratios. The shear force is transferred by the concrete strut to the supports directly by reducing the a/d ratio. When examining the average ratios at the upper and lower boundary of the limit values for each method, 8%, 14% and 18% differences were obtained for the ANN, EL and ACI318-14-STM methods, respectively (Fig. 9).

In this study, 0.003 was considered as the limit value of the horizontal and vertical web reinforcement ratio according to the strut-and-tie model approach in ACI318-14-chapter 23. Approximately the same average $V_{n,test}/V_{n,estimated}$ ratios had been obtained at the upper and lower boundary of the limit values for all calculation methods. When comparing the methods on their own, horizontal web reinforcement ratio with 3%, 9% and 18% differences were obtained for the ANN, EL and ACI318-14-STM methods, respectively (Fig. 10). Vertical web reinforcement ratios with 1%, 8% and 17% differences were obtained for the ANN, EL and ACI318-14-STM methods, respectively (Fig. 11).

When examining the results in general, the closest results were obtained from the ANN model. The similar average values were obtained for the ANN, ACI318-14-STM and EL methods for the selected upper and lower limit values of the horizontal and vertical web reinforcement ratios.

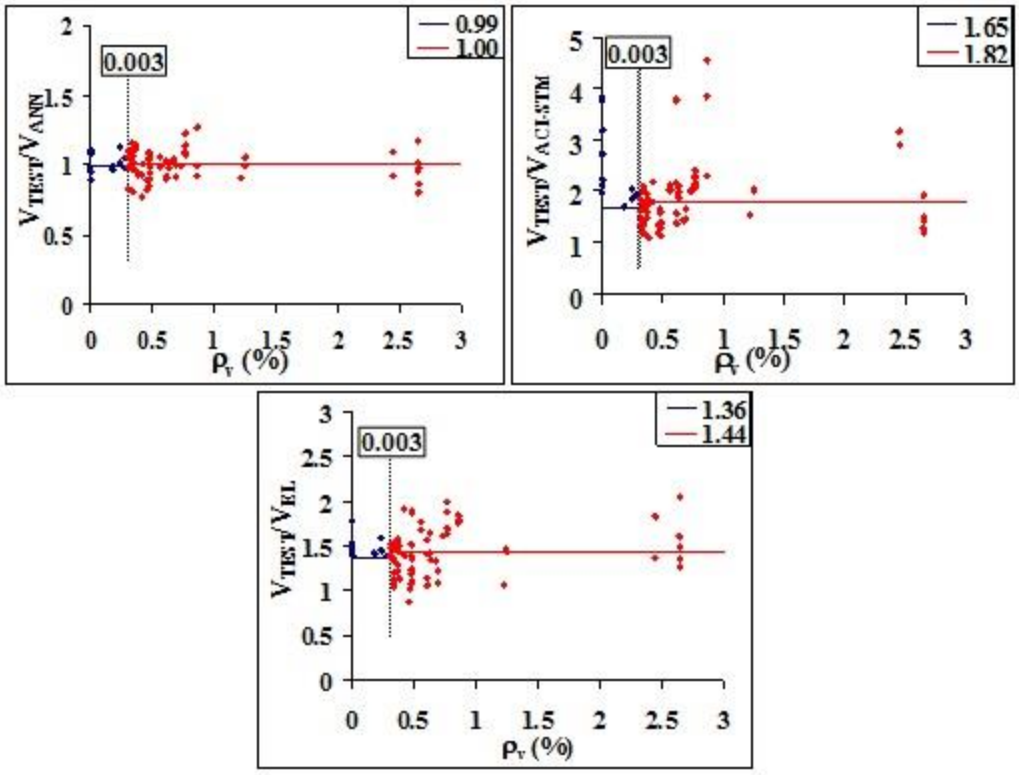

Fig. 11 Effect of the parameter ρ_v on the shear strength of the RC deep beams

6. Conclusions

In this paper, an ANN model was developed for the estimation of the shear capacities of the RC deep beams. In this study, to analyze the performance of the proposed ANN model, 214 different RC deep beam tests were collected from the literature, and the testing and training of the ANN model were performed. Next, the success of the proposed ANN method compared to the conventional code approaches was investigated. The following conclusions may be drawn based on the results presented:

- The results obtained from the testing/training data set of the proposed ANN model were satisfactory (the accuracy rate was calculated as 97%). Furthermore, the ANN model showed a slight improvement in performance compared with the EL approach.
- In the present study, the data sets used were similar to the data sets used by Park and Kuchma (2007), and an ANN model was developed. In the abovementioned study (Park and Kuchma, 2007), a strut-and-tie based method was presented for calculating the strength of the reinforced concrete deep beams. This method was compared with the strut-and-tie provisions in the ACI318 code. Therefore, the accuracy rate obtained is different from that of the above study.
- In the ANN approach, the selected algorithm and the data set used in the training stage directly affects the accuracy and speed of the test results. The selection of the appropriate algorithm for the data set is as significant a parameter as the optimum hidden nodes, the iteration number, the learning rate, the momentum constant and the error tolerance.

• The performance of the developed ANN model was limited to the range of the input data used in the training and testing processes, but the model can easily be developed with additional new sets of data. The developed ANN model should be used to predict the shear strength of the deep beams within the range of different parameters in the database.
• All selected parameters affect the shear strength capacity of the RC deep beams. However, the current building code mentioned in the text is quite limited in predicting the shear strength of an RC deep beam because several parameters are ignored, such as the longitudinal reinforcement bar ratio (ρ).
• The test results are greater than the values obtained from the ACI318-14-STM and EL methods. The test results were 1.76 times the values for the ACI318-14-STM method and 1.41 times those for the EL method as average values (for all database tests), which is expected because the codes are very conservative. In particular, the shear strength values of the deep beams obtained from the ACI318-14-STM method were very different from the experimental strengths, as clearly demonstrated by the average ratios. The test results were 0.99 times the values for the ANN method as average values (for testing data).
• Generally, the ACI318-14-STM and EL results were smaller than the experimental shear strengths except for the ANN model. This scenario showed that the ACI318-14-STM method is more conservative, as expected and the building code is limited in predicting the shear strength of an RC deep beam. Moreover, several parameters that affect shear strength are ignored in the current codes.
• In all RMSE, MAE and MAPE performance parameters, the best values were obtained in ANN model. Although R^2 values which obtained from ACI318-14-STM code and EL were highest values, in other performance parameters the obtained values were not satisfied the R^2 values.

References

ACI318-05 (2005), *Building Code Requirements for Structural Concrete and Commentary*, American Concrete Institute, Farmington Hills, MI, USA.

ACI318-14 (2014), *Building Code Requirements for Structural Concrete and Commentary*, American Concrete Institute, Farmington Hills, MI, USA.

Aguilar, G., Matamoros, A.B., Parra-Montesinos, G., Ramirez, J.A. and Wight, J.K. (2002), "Experimental evaluation of design procedures for shear strength of deep reinforced concrete beams", *ACI Struct. J.*, **99**(4), 539-548.

Akbas, B. (2006), "A neural network model to assess the hysteretic energy demand in steel moment resisting frames", *Struct. Eng. Mech.*, **23**(2), 177-193.

Anderson, N.S. and Ramirez, J.A. (1989), "Detailing of stirrup reinforcement", *ACI Struct. J.*, **86**(5), 507-515.

Arslan, M.H., Ceylan, M., Kaltakci, M.Y., Ozbay, Y. and Gulay, G. (2007), "Prediction of force reduction factor R of prefabricated ındustrial buildings using neural networks", *Struct. Eng. Mech*., **27**(2), 117-134.

Arslan M.H. (2009), "Application of ANN to evaluate effective parameters affecting failure load and displacement of RC buildings", *Nat Hazard. Earth. Syst. Sci.*, **9**, 967-977.

Arslan, M.H. (2010), "An evaluation of effective design parameters on earthquake performance of RC buildings using neural networks", *Eng. Struct.*, **32**, 1888-1898.

Chen, H.M., Tsai, K.H., Qi, G.Z., Yang, J.C.S. and Amini, F. (1995), "Neural networks for structural control", *J. Comput. Civil Eng.*, **9**(2), 168-176.

Chetchotisak, P., Teerawong, J., Yindeesuk, S. and Song, J. (2014), "New strut-and-tie models for shear

strength prediction and design of RC deep beams", *Comput. Concrete*, **14**(1), 19-40.
Clark, A.P. (1951), "Diagonal tension in reinforced concrete beams", *ACI J.*, **48**(10), 145-156.
CSA A23.3-04 (2004), *Design of Concrete Structures*, Canadian Standards Association, Canada.
Elcordy, M.F., Chang, K.C. and Lee, G.C. (1993), "Neural networks trained by analytically simulated damage states", *J. Comput. Civil Eng.*, **7**(2), 130-145.
Eun, H.C., Lee, Y.H., Chung, H.S. and Yang, K.H. (2006), "On the shear strength of reinforced concrete deep beam with web opening", *Struct. Des. Tall Spec. Build.*, **15**, 445-466.
Eurocode 2 (2004), *Design of concrete structures*, European Committee for Standardization.
Fu, L. (1994), *Neural Networks in Computer Intelligence*, McGraw-Hill: USA.
Inel, M. (2007), "Modeling ultimate deformation capacity of RC columns using artificial neural networks", *Eng. Struct.*, **29**(3), 329-335.
Kong, F.K., Robins, P.J. and Cole, D.F. (1970), "Web reinforcement effects on deep beams", *ACI J.*, **67**(12), 1010-1017.
Lautour, O.R. and Omenzetter, P. (2009), "Prediction of seismic-induced structural damage using artificial neural networks", *Eng. Struct.*, **31**, 600-606.
MacGregor, J.G. (1997), *Reinforced Concrete Mechanics and Design*, 3rd Edition, Prentice-Hall International Inc., New Jersey.
MATLAB (2006), *Neural Network Toolbox User Guide*, Matrix Laboratory.
Mohammadhassani, M., Saleh A., Suhatril, M. and Safa, M. (2015), "Fuzzy modelling approach for shear strength prediction of RC deep beams", *Smart Struct. Syst.*, **16**(3), 497-519.
Oh, J.K. and Shin, S.W. (2001), "Shear strength of reinforced high-strength concrete deep beams", *ACI Struct. J.*, **98**(2), 164-173.
Ozturk, M. (2012), "Prediction of tensile capacity of adhesive anchors including edge and group effects using neural networks", *Sci. Eng. Compos. Mater.*, **20**(1), 95-104.
Park, J.W. and Kuchma, D. (2007), "Strut-and-tie model analysis for strength prediction of deep beams", *ACI Struct. J.*, **104**(6), 657-666.
Quintero-Febres, C.G., Parra-Montesinos, G. and Wight, J.K. (2006), "Strength of struts in deep concrete members designed using strut-and-tie method", *ACI Struct. J.*, **103**(4), 577-586.
Schlaich, J., Schafer, K. and Jennewein, M. (1987), "Toward a consistent design of structural concrete", *PCI J.*, **32**(3), 74-150.
Smith, K.N. and Vantsiotis, A.S. (1982), "Shear strength of deep beams", *ACI J.*, **79**(3), 201-213.
Tan, K.H., Kong, F.K., Teng, S. and Guan, L. (1995), "High-strength concrete deep beams with effective span and shear span variations", *ACI Struct. J.*, **92**(4), 395-405.
Williams, D.E., Rumelhart, G.E., Hinton, R.J. and Hinton, G. (1986), "Learning representations by back-propagating errors", *Nature*, **323**, 533-536.
Yang, K.H., Ashour, A., Song, J.K. and Lee, E.T. (2008), "Neural network modelling of RC deep beam shear strength", *Proc. Inst. Civil Eng. Struct. Build.*, **161**(SB1), 29-39.
Yavuz, G., Arslan, M.H. and Baykan, O.K. (2014), "Shear strength predicting of FRP-strengthened RC beams by using artificial neural networks", *Sci. Eng. Compos. Mater.*, **21**(2), 239-255.

CC

Notations

a/d : aspect ratio
A_{si} : area of reinforcement crossing the strut
b_w : beam web width
c : concrete cover

d : effective depth
$f_c^{'}$: specified concrete compressive strength
h : height of beam
jd : distance between the centre of top and bottom nodes
l_b : width of loading plates
s_i : spacing of reinforcement crossing the strut
w_s : width of concrete strut
w_t : depth of bottom node
V_n : Shear strength
β_s : effectiveness factor of concrete
ρ : ratio of longitudinal reinforcement
ρ_h : ratio of horizontal web reinforcement
ρ_v : ratio of vertical web reinforcement
α_i : angle between reinforcing bar j and the axis of beam
θ_s : concrete strut angle

Appendix

Appendix Table Geometrical and mechanical characteristics of the RC deep beams (Park and Kuchma 2007)

Reference	Specimen no	f_c' (MPa)	b (mm)	h (mm)	d (mm)	a (mm)	a/d	ρ	ρ_h	ρ_v
Smith and Vantsiotis (1982)	0A0-44	20.5	102	356	305	305	1.00	1.94	0	0
	0A0-48	20.9	102	356	305	305	1.00	1.94	0	0
	1A1-10	18.7	102	356	305	305	1.00	1.94	0.23	0.28
	1A3-11	18	102	356	305	305	1.00	1.94	0.45	0.28
	1A4-12	16.1	102	356	305	305	1.00	1.94	0.68	0.28
	1A4-51	20.5	102	356	305	305	1.00	1.94	0.68	0.28
	1A6-37	21.1	102	356	305	305	1.00	1.94	0.91	0.28
	2A1-38	21.7	102	356	305	305	1.00	1.94	0.23	0.63
	2A3-39	19.8	102	356	305	305	1.00	1.94	0.45	0.63
	2A4-40	20.3	102	356	305	305	1.00	1.94	0.68	0.63
	2A6-41	19.1	102	356	305	305	1.00	1.94	0.91	0.63
	3A1-42	18.4	102	356	305	305	1.00	1.94	0.23	1.25
	3A3-43	19.2	102	356	305	305	1.00	1.94	0.45	1.25
	3A4-45	20.8	102	356	305	305	1.00	1.94	0.68	1.25
	3A6-46	19.9	102	356	305	305	1.00	1.94	0.91	1.25
	0B0-49	21.7	102	356	305	368	1.21	1.94	0	0
	1B1-01	22.1	102	356	305	368	1.21	1.94	0.23	0.24
	1B3-29	20.1	102	356	305	368	1.21	1.94	0.45	0.24
	1B4-30	20.8	102	356	305	368	1.21	1.94	0.68	0.24
	1B6-31	19.5	102	356	305	368	1.21	1.94	0.91	0.24
	2B1-05	19.2	102	356	305	368	1.21	1.94	0.23	0.42
	2B3-06	19	102	356	305	368	1.21	1.94	0.45	0.42
	2B4-07	17.5	102	356	305	368	1.21	1.94	0.68	0.42
	2B4-52	21.8	102	356	305	368	1.21	1.94	0.68	0.42
	2B6-32	19.8	102	356	305	368	1.21	1.94	0.91	0.42
	3B1-08	16.2	102	356	305	368	1.21	1.94	0.23	0.63
	3B1-36	20.4	102	356	305	368	1.21	1.94	0.23	0.77
	3B3-33	19	102	356	305	368	1.21	1.94	0.45	0.77
	3B4-34	19.2	102	356	305	368	1.21	1.94	0.68	0.77
	3B6-35	20.6	102	356	305	368	1.21	1.94	0.91	0.77
	4B1-09	17.1	102	356	305	368	1.21	1.94	0.23	1.25
	0C0-50	20.7	102	356	305	457	1.50	1.94	0	0
	1C1-14	19.2	102	356	305	457	1.50	1.94	0.23	0.18
	1C3-02	21.9	102	356	305	457	1.50	1.94	0.45	0.18
	1C4-15	22.7	102	356	305	457	1.50	1.94	0.68	0.18
	1C6-16	21.8	102	356	305	457	1.50	1.94	0.91	0.18
	2C1-17	19.9	102	356	305	457	1.50	1.94	0.23	0.31

Appendix Table Continued

Reference	Specimen no	*fc'* (MPa)	*b* (mm)	*h* (mm)	*d* (mm)	*a* (mm)	*a/d*	ρ	ρ_h	ρ_v
Smith and Vantsiotis (1982)	2C3-03	19.2	102	356	305	457	1.50	1.94	0.45	0.31
	2C3-27	19.3	102	356	305	457	1.50	1.94	0.45	0.31
	2C4-18	20.4	102	356	305	457	1.50	1.94	0.68	0.31
	2C6-19	20.8	102	356	305	457	1.50	1.94	0.91	0.31
	3C1-20	21	102	356	305	457	1.50	1.94	0.23	0.56
	3C3-21	16.5	102	356	305	457	1.50	1.94	0.45	0.56
	3C4-22	18.3	102	356	305	457	1.50	1.94	0.68	0.56
	3C6-23	19	102	356	305	457	1.50	1.94	0.91	0.56
	4C1-24	19.6	102	356	305	457	1.50	1.94	0.23	0.77
	4C3-04	18.5	102	356	305	457	1.50	1.94	0.45	0.63
	4C3-28	19.2	102	356	305	457	1.50	1.94	0.45	0.77
	4C4-25	18.5	102	356	305	457	1.50	1.94	0.68	0.77
	4C6-26	21.2	102	356	305	457	1.50	1.94	0.91	0.77
	0D0-47	19.5	102	356	305	635	2.08	1.94	0	0
	4D1-13	16.1	102	356	305	635	2.08	1.94	0.23	0.42
Kong *et al.* (1970)	1-30	21.5	76	762	724	254	0.35	0.52	0	2.45
	1-25	24.6	76	635	597	254	0.43	0.62	0	2.45
	1-20	21.2	76	508	470	254	0.54	0.79	0	2.45
	1-15	21.2	76	381	343	254	0.74	1.09	0	2.45
	1-10	21.7	76	254	216	254	1.18	1.73	0	2.45
	2-30	19.2	76	762	724	254	0.35	0.52	0	0.86
	2-25	18.6	76	635	597	254	0.43	0.62	0	0.86
	2-20	19.9	76	508	470	254	0.54	0.79	0	0.86
	2-15	22.8	76	381	343	254	0.74	1.09	0	0.86
	2-10	20.1	76	254	216	254	1.18	1.73	0	0.86
	3-30	22.6	76	762	724	254	0.35	0.52	2.45	0
	3-25	21	76	635	597	254	0.43	0.62	2.45	0
	3-20	19.2	76	508	470	254	0.54	0.79	2.45	0
	3-15	21.9	76	381	343	254	0.74	1.09	2.45	0
	3-10	22.6	76	254	216	254	1.18	1.73	2.45	0
	4-30	22	76	762	724	254	0.35	0.52	0.86	0
	4-25	21	76	635	597	254	0.43	0.62	0.86	0
	4-20	20.1	76	508	470	254	0.54	0.79	0.86	0
	4-15	22	76	381	343	254	0.74	1.09	0.86	0
	4-10	22.6	76	254	216	254	1.18	1.73	0.86	0
	5-30	18.6	76	762	724	254	0.35	0.52	0.61	0.61
	5-25	19.2	76	635	597	254	0.43	0.62	0.61	0.61
	5-20	20.1	76	508	470	254	0.54	0.79	0.61	0.61
	5-15	21.9	76	381	343	254	0.74	1.09	0.61	0.61
	5-10	22.6	76	254	216	254	1.18	1.73	0.61	0.61

Appendix Table Continued

Reference	Specimen no	*fc'* (MPa)	*b* (mm)	*h* (mm)	*d* (mm)	*a* (mm)	*a/d*	ρ	ρ_h	ρ_v
Clark (1951)	A1-1	24.6	203	457	390	914	2.34	3.1	0	0.38
	A1-2	23.6	203	457	390	914	2.34	3.1	0	0.38
	A1-3	23.4	203	457	390	914	2.34	3.1	0	0.38
	A1-4	24.8	203	457	390	914	2.34	3.1	0	0.38
	B1-1	23.4	203	457	390	762	1.95	3.1	0	0.37
	B1-2	25.4	203	457	390	762	1.95	3.1	0	0.37
	B1-3	23.7	203	457	390	762	1.95	3.1	0	0.37
	B1-4	23.3	203	457	390	762	1.95	3.1	0	0.37
	B1-5	24.6	203	457	390	762	1.95	3.1	0	0.37
	B2-1	23.2	203	457	390	762	1.95	3.1	0	0.73
	B2-2	26.3	203	457	390	762	1.95	3.1	0	0.73
	B2-3	24.9	203	457	390	762	1.95	3.1	0	0.73
	B6-1	42.1	203	457	390	762	1.95	3.1	0	0.37
	C1-1	25.6	203	457	390	610	1.56	2.07	0	0.34
	C1-2	26.3	203	457	390	610	1.56	2.07	0	0.34
	C1-3	24	203	457	390	610	1.56	2.07	0	0.34
	C1-4	29	203	457	390	610	1.56	2.07	0	0.34
	C2-1	23.6	203	457	390	610	1.56	2.07	0	0.69
	C2-2	25	203	457	390	610	1.56	2.07	0	0.69
	C2-3	24.1	203	457	390	610	1.56	2.07	0	0.69
	C2-4	27	203	457	390	610	1.56	2.07	0	0.69
	C3-1	14.1	203	457	390	610	1.56	2.07	0	0.34
	C3-2	13.8	203	457	390	610	1.56	2.07	0	0.34
	C3-3	13.9	203	457	390	610	1.56	2.07	0	0.34
	C4-1	24.5	203	457	390	610	1.56	3.1	0	0.34
	C6-2	45.2	203	457	390	610	1.56	3.1	0	0.34
	C6-3	44.7	203	457	390	610	1.56	3.1	0	0.34
	C6-4	47.6	203	457	390	610	1.56	3.1	0	0.34
	D1-1	26.2	203	457	390	457	1.17	1.63	0	0.46
	D1-2	26.1	203	457	390	457	1.17	1.63	0	0.46
	D1-3	24.5	203	457	390	457	1.17	1.63	0	0.46
Clark (1951)	D2-1	24	203	457	390	457	1.17	1.63	0	0.61
	D2-2	25.9	203	457	390	457	1.17	1.63	0	0.61
	D2-3	24.8	203	457	390	457	1.17	1.63	0	0.61
	D2-4	24.5	203	457	390	457	1.17	1.63	0	0.61
	D3-1	28.2	203	457	390	457	1.17	2.44	0	0.92
	D4-1	23.1	203	457	390	457	1.17	1.63	0	1.22

Appendix Table Continued

Reference	Specimen no	*fc'* (MPa)	*b* (mm)	*h* (mm)	*d* (mm)	*a* (mm)	*a/d*	ρ	ρ_h	ρ_v
	N4200	23.7	130	560	500	425	0.85	1.56	0	0
	N42A2	23.7	130	560	500	425	0.85	1.56	0.43	0.12
	N42B2	23.7	130	560	500	425	0.85	1.56	0.43	0.22
	N42C2	23.7	130	560	500	425	0.85	1.56	0.43	0.34
	H4100	49.1	130	560	500	250	0.50	1.56	0	0
	H41A2(1)	49.1	130	560	500	250	0.50	1.56	0.43	0.12
	H41B2	49.1	130	560	500	250	0.50	1.56	0.43	0.22
	H41C2	49.1	130	560	500	250	0.50	1.56	0.43	0.34
	H4200	49.1	130	560	500	425	0.85	1.56	0	0
	H42A2(1)	49.1	130	560	500	425	0.85	1.56	0.43	0.12
	H42B2(1)	49.1	130	560	500	425	0.85	1.56	0.43	0.22
	H42C2(1)	49.1	130	560	500	425	0.85	1.56	0.43	0.34
	H4300	49.1	130	560	500	625	1.25	1.56	0	0
	H43A2(1)	49.1	130	560	500	625	1.25	1.56	0.43	0.12
	H43B2	49.1	130	560	500	625	1.25	1.56	0.43	0.22
	H43C2	49.1	130	560	500	625	1.25	1.56	0.43	0.34
	H4500	49.1	130	560	500	1000	2.00	1.56	0	0
	H45A2	49.1	130	560	500	1000	2.00	1.56	0.43	0.12
	H45B2	49.1	130	560	500	1000	2.00	1.56	0.43	0.22
Oh and Shin (2001)	H45C2	49.1	130	560	500	1000	2.00	1.56	0.43	0.34
	H41A0	50.7	120	560	500	250	0.50	1.29	0	0.13
	H41A1	50.7	120	560	500	250	0.50	1.29	0.23	0.13
	H41A2(2)	50.7	120	560	500	250	0.50	1.29	0.47	0.13
	H41A3	50.7	120	560	500	250	0.50	1.29	0.94	0.13
	H42A2(2)	50.7	120	560	500	425	0.85	1.29	0.47	0.13
	H42B2(2)	50.7	120	560	500	425	0.85	1.29	0.47	0.24
	H42C2(2)	50.7	120	560	500	425	0.85	1.29	0.47	0.37
	H43A0	50.7	120	560	500	625	1.25	1.29	0	0.13
	H43A1	50.7	120	560	500	625	1.25	1.29	0.23	0.13
	H43A2(2)	50.7	120	560	500	625	1.25	1.29	0.47	0.13
	H43A3	50.7	120	560	500	625	1.25	1.29	0.94	0.13
	H45A2(2)	50.7	120	560	500	1000	2.00	1.29	0.46	0.13
	U41A0	73.6	120	560	500	250	0.50	1.29	0	0.13
	U41A1	73.6	120	560	500	250	0.50	1.29	0.23	0.13
	U41A2	73.6	120	560	500	250	0.50	1.29	0.47	0.13
	U41A3	73.6	120	560	500	250	0.50	1.29	0.94	0.13
	U42A2	73.6	120	560	500	425	0.85	1.29	0.47	0.13
	U42B2	73.6	120	560	500	425	0.85	1.29	0.47	0.24
	U42C2	73.6	120	560	500	425	0.85	1.29	0.47	0.37

Appendix Table Continued

Reference	Specimen no	*fc'* (MPa)	*b* (mm)	*h* (mm)	*d* (mm)	*a* (mm)	*a/d*	ρ	ρ_h	ρ_v
Oh and Shin (2001)	U43A0	73.6	120	560	500	625	1.25	1.29	0	0.13
	U43A1	73.6	120	560	500	625	1.25	1.29	0.23	0.13
	U43A2	73.6	120	560	500	625	1.25	1.29	0.47	0.13
	U43A3	73.6	120	560	500	625	1.25	1.29	0.94	0.13
	U45A2	73.6	120	560	500	1000	2.00	1.29	0.47	0.13
	N33A2	23.7	130	560	500	625	1.25	1.56	0.43	0.12
	N43A2	23.7	130	560	500	625	1.25	1.56	0.43	0.12
	N53A2	23.7	130	560	500	625	1.25	1.56	0.43	0.12
	H31A2	49.1	130	560	500	250	0.50	1.56	0.43	0.12
	H32A2	49.1	130	560	500	425	0.85	1.56	0.43	0.12
	H33A2	49.1	130	560	500	625	1.25	1.56	0.43	0.12
Oh and Shin (2001)	H51A2	49.1	130	560	500	250	0.50	1.56	0.43	0.12
	H52A2	49.1	130	560	500	425	0.85	1.56	0.43	0.12
	H53A2	49.1	130	560	500	625	1.25	1.56	0.43	0.12
Aguilar *et al.* (2002)	ACI-I	32	305	915	791	915	1.16	1.27	0.35	0.31
	STM-I	32	305	915	718	915	1.27	1.4	0.13	0.31
	STM-H	28	305	915	801	915	1.14	1.25	0.06	0.31
	STM-M	28	305	915	801	915	1.14	1.25	0	0.1
Quintero-Febres *et al.* (2006)	A1	22	150	460	370	525	1.42	2.79	0.1	0.28
	A2	22	150	460	370	525	1.42	2.79	0.1	0.28
	A3	22	150	460	370	525	1.42	2.79	0	0
	A4	22	150	460	370	525	1.42	2.79	0	0
	B1	32.4	150	460	375	334	0.89	2.04	0.1	0.23
	B2	32.4	150	460	375	334	0.89	2.04	0.1	0.23
	B3	32.4	150	460	375	304	0.81	2.04	0	0
	B4	32.4	150	460	375	304	0.81	2.04	0	0
	HA1	50.3	100	460	380	597	1.57	4.08	0.15	0.38
	HA3	50.3	100	460	380	543	1.43	4.08	0	0
	HB1	50.3	100	460	380	342	0.90	4.08	0.15	0.67
	HB3	50.3	100	460	380	312	0.82	4.08	0	0
Tan *et al.* (1995)	A-0.27-2.15	58.8	110	500	463	125	0.27	1.23	0	0.48
	A-0.27-3.23	51.6	110	500	463	125	0.27	1.23	0	0.48
	A-0.27-4.30	53.9	110	500	463	125	0.27	1.23	0	0.48
	A-0.27-5.38	57.3	110	500	463	125	0.27	1.23	0	0.48
	B-0.54-2.15	56	110	500	463	250	0.54	1.23	0	0.48
	B-0.54-3.23	45.7	110	500	463	250	0.54	1.23	0	0.48
	B-0.54-4.30	53.9	110	500	463	250	0.54	1.23	0	0.48
	B-0.54-5.38	53	110	500	463	250	0.54	1.23	0	0.48
	C-0.81-2.15	51.2	110	500	463	375	0.81	1.23	0	0.48

Appendix Table Continued

Reference	Specimen no	*fc'* (MPa)	*b* (mm)	*h* (mm)	*d* (mm)	*a* (mm)	*a/d*	ρ	ρ_h	ρ_v
Tan *et al.* (1995)	C-0.81-3.23	44	110	500	463	375	0.81	1.23	0	0.48
	D-1.08-2.15	48.2	110	500	463	500	1.08	1.23	0	0.48
	D-1.08-3.23	44.1	110	500	463	500	1.08	1.23	0	0.48
	D-1.08-4.30	46.8	110	500	463	500	1.08	1.23	0	0.48
	D-1.08-5.38	48	110	500	463	500	1.08	1.23	0	0.48
	E-1.62-3.23	50.6	110	500	463	750	1.62	1.23	0	0.48
	E-1.62-4.30	44.6	110	500	463	750	1.62	1.23	0	0.48
	E-1.62-5.38	45.3	110	500	463	750	1.62	1.23	0	0.48
	F-2.16-4.30	41.1	110	500	463	1000	2.16	1.23	0	0.48
	G-2.70-5.38	42.8	110	500	463	1250	2.70	1.23	0	0.48
Anderson and Ramirez (1989)	1	39	203	508	425	914	2.15	2.67	0	2.65
	2	41.4	203	508	425	914	2.15	2.67	0	2.65
	3	42.7	203	508	425	914	2.15	2.67	0	2.65
	4	27.5	203	508	425	914	2.15	2.67	0	2.65
	5	28.7	203	508	425	914	2.15	2.67	0	2.65
	6	29.4	203	508	425	914	2.15	2.67	0	2.65
	7	32.1	203	508	425	914	2.15	2.67	0	2.65
	8	33.9	203	508	425	914	2.15	2.67	0	2.65
	9	34.4	203	508	425	914	2.15	2.67	0	2.65
	10	31	203	508	425	914	2.15	2.67	0	2.65
	11	32.3	203	508	425	914	2.15	2.67	0	2.65
	12	33.2	203	508	425	914	2.15	2.67	0	2.65